The different anion transport capability of prodiginine- and tambjamine-like molecules

Michele Fiore[1], María García-Valverde[2], Israel Carreira-Barral[2] and Oscar Moran[1]

[1]Istituto di Biofisica, CNR, Genova, Italy; [2]Departamento de Química, Facultad de Ciencias, Universidad de Burgos, Burgos, Spain

Correspondence:
Michele Fiore
Istituto di Biofisica, CNR
via De Marini, 6 16149 Genova, Italy.
Email: fiore@ge.ibf.cnr.it

Abstract

Prodiginines and tambjamines are anion-selective ionophores capable of facilitating the transport of anions across the plasma membrane in mammalian cells. One of the potential applications of these anionophores is the possibility of employing them as a substitutive therapy for pathologies involving anion channels, as in cystic fibrosis. We have studied the interaction of a large anion as gluconate with three prodiginine- and two tambjamine-like compounds. Apparent dissociation constants for the chloride, iodide and gluconate complexes were estimated from iodide influx experiments in mammalian cells exposed to different extracellular anion combinations. Our experiments indicate that gluconate is not transported by the prodiginines, leaving the anionophores free to transport chloride and iodide. Conversely, gluconate would be transported to some extent by the tambjamines, competing with halides for the anionophores, and consequently reducing their flux. This might be related to the different structural features of both families of compounds. These data have important implications for the selection of impermeable anions in the analysis of the anionophore mechanism.

Keywords: anionophore, anion transport, anion binding, prodiginine, tambjamine

1. Introduction

Anionophores are natural molecules produced by living organisms capable of facilitating anion transport through the cell membrane. Among the different molecules able to carry anions, we have focused on some prodiginine and tambjamine derivatives. Prodiginines take their name from Prodigiosin, a red bacterial pigment secreted by *Serratia marcescens* (Yip et al. 2019), whereas tambjamines are secondary metabolites isolated from soft-bodied marine gastropod mollusks. Both groups of molecules play an important role in defense mechanisms (Carté and Faulkner 1986). Inspired by their characteristics, a large number of anionophores has been developed and reported in the literature (Hernando et al. 2018; Gale, Davis, and Quesada 2017; Carreira-Barral et al. 2019). In our laboratories, we have demonstrated that prodiginine- and tambjamine-like compounds can transport biologically relevant anions, such as chloride and bicarbonate, through artificial phospholipid bilayers and mammalian cell membranes (Cossu et al. 2018; Hernando et al. 2018; Davis, Okunola, and Quesada 2010; Fiore et al. 2019; Caci et al. 2020). Among the potential applications of these anionophores perhaps the most striking one is the possibility of employing them as a new therapeutic approach for pathologies involving anion channels or transporters, as it happens in cystic fibrosis. Indeed, we have proven that both prodiginine- and tambjamine-like molecules can transport anions (chloride, iodide and bicarbonate) across the plasma membrane in mammalian cells in amounts comparable to the wild-type CFTR protein. Furthermore, we have also observed that some of these derivatives possess low cytotoxicity, thus indicating them as eligible for further development as drugs (Fiore et al. 2019; Caci et al. 2020).

We have previously reported that the interaction of large hydrophilic anions, such as gluconate, with prodiginines and tambjamines, is remarkably different (Fiore et al. 2019). In this work, we have investigated the transport properties of five different anionophores belonging to those families by iodide influx experiments in mammalian cells. Anion substitutions in the extracellular solution

allowed us to propose a kinetic model for the binding of the studied anions (chloride, iodide and gluconate) to the carriers, suggesting important differences about anion interaction in both families of compounds. This investigation is complemented with a structural study both of the anionophores and the anionophore-anion complexes, conducted by means of computational calculations.

2. Methods

2.1 Anionophores

We assayed three prodiginines, prodigiosine, PRG (Rapoport and Holden, 1962), Obatoclax, OBX, (Díaz de Greñu et al., 2011) and EH130 (Hernando et al., 2018), and two tambjamines, MM3 (Hernando et al., 2014) and RQ363 (Fiore et al., 2019). Pure (>98%) anionophores were dissolved in DMSO at a concentration of 345 mM and kept at -20 °C. A fresh aliquot of the anionophore solution was diluted in the working solution immediately before the experiment.

2.2 Iodide influx assay

Fisher Rat Thyroid (FRT) cells stably transfected with a halide-sensitive yellow fluorescence protein, H148Q/I152L-YFP (Galietta, Haggie, and Verkman 2001), were grown at 37 °C and 5% CO_2 in modified F12 Coon's medium with addition of 10% FBS, 2 mM of glutamine, 1 mg/ml of penicillin and 100 µg/ml of streptomycin. Besides, hygromycin was added as a selective agent for stable YFP-transfected clones. Cells were seeded in 96-well microplates at a density of 40,000 cells/ well. The experiments were carried out 48 hours after seeding.

To determine the transport activity of the selected anionophores, we measured the influx of iodide that caused the quenching of the YFP inside the cell. The fluorescence of the YFP was monitored using a fluorescence plate reader (Tristar2 S, Berthold Technologies, Bad Wildbad, Germany) equipped with 485 nm excitation and 535 nm emission filters (Fiore et al. 2019). Cells were incubated for 30 minutes at 37 °C in a solution containing (in mM): KNO_3 4.5, $Ca(NO_3)_2$ 1.2, $MgSO_4$ 0.2, Glucose 5, HEPES 20, pH 7.4, NaCl 136. To obtain different concentrations of the anions, NaCl was isomolarly replaced by NaGluconate. The incubation solution also contained 2 µM of the corresponding anionophore or the vehicle DMSO (≤0.5% v/v), in a final volume of 60 µL.

After recording the fluorescence for 5 seconds (baseline), 100 µL of a solution where NaCl (or NaGluconate) had been replaced by NaI were injected in the wells, and the emission was monitored for 60 seconds more. In this way, the final concentration of NaI was 85 mM, and the sum of the NaCl and NaGluconate concentrations was 51 mM. Measurements were performed at 37 °C, and the fluorescence during the experiments was recorded every 0.2 seconds.

The fluorescence time course was normalized to the average of the fluorescence of the baseline recorded before NaI injection. The initial rate of fluorescence decay (QR) was derived by fitting the signal to a double exponential function. The QR is an indicator of the iodide influx, and therefore of the anionophores activity (Fiore et al. 2019; Galietta, Haggie, and Verkman 2001). Measurements were repeated 5 to 9 times at each experimental condition.

2.3 Structure analysis

Calculations of the electronic molecular structures were performed using the Gaussian 09 program (Frisch et al. 2016). The geometries of all species were fully optimized at the B3LYP/DGTZVP level. Optimizations were carried out assuming the environmental parameters describing the corresponding molecule in water, taken into account by the Polarisable Continuum Model (PCM) using the CPCM model (Cossi et al. 2003; Barone and Cossi 1998). The nature of all optimized structures was determined by using harmonic frequency analysis as true minima with no imaginary frequencies.

3. Results

The iodide transport to the intracellular compartment was measured as the initial fluorescence quenching rate (QR) in FRT cells expressing the halide-sensitive YFP. This preparation is well standardized for halide transport measurement (Galietta et al 2001), and has been previously used for determine the transport characteristics of anionophores (Cossu et al. 2018, Hernando et al. 2018, Fiore et al 2019). Iodide transport in cells incubated with 0.5% DMSO, the vehicle used for the anionophores, was very small, and it is probably due to endogenous mechanisms present in FRT cells (Figure 1A). Differently, when cells were incubated in solutions with 2 μM of the anionophores we observed a significant iodide influx, as shown in Figures 1B-F. Interestingly, as displayed in Figures 1B-D, for the three prodiginines assayed the substitution of chloride (black trace) by gluconate (red trace) causes an increase of the iodide influx. However, when it comes to the tambjamines such replacement leads to a reduction of the influx (Figures 1E-F).

Anion competition model

We hypothesized that the anionic composition of the extracellular solution influences the anionophore-driven transport due to a competition of the different anion species for the carrier's binding site. Consistently with what is observed in Figures 1B-D, when chloride is replaced by gluconate, there is an increase of iodide transport in those cells incubated with prodiginines PRG, OBX and EH130. These phenomena can be interpreted as the competition of two anions, chloride and iodide, for a single binding site in the anionophore:

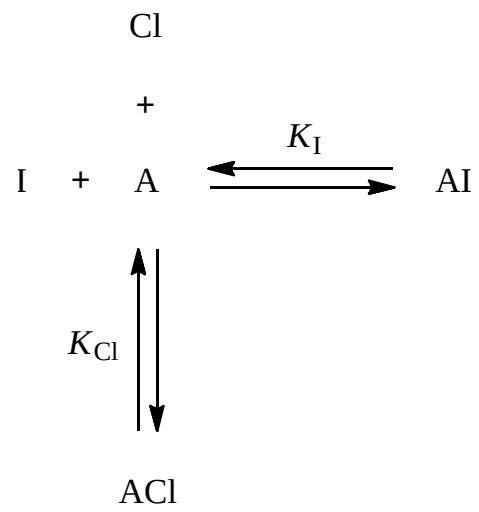

where A is the free, unbound anionophore and ACl and AI represent the anionophore-chloride and anionophore-iodide complexes, respectively. In this scheme, gluconate does not interact with the anionophore. The apparent dissociation constants, K_{Cl} and K_I, for the two complexes are defined by:

$$K_{Cl}=\frac{\mathrm{Cl}\times\mathrm{A}}{\mathrm{ACl}};\ K_I=\frac{\mathrm{I}\times\mathrm{A}}{\mathrm{AI}};\ \mathrm{A}+\mathrm{AI}+\mathrm{ACl}=1 \quad (1)$$

As iodide has a significantly higher affinity for the H148Q/I152L-YFP than chloride (reference), we assume that the QR is reflecting mostly the iodide influx, and therefore it should describe the formation of the AI complex. Thus, solving the equations in (1) for AI we have:

$$K_I=\frac{\mathrm{I}\times\mathrm{A}}{\mathrm{AI}} \quad (2)$$

where AI_{max} is the maximum QR expected in the absence of chloride.

On the contrary, as displayed in Figures 1E-F, when cells are incubated in the presence of tambjamine derivatives MM3 and RQ363, the replacement of chloride by gluconate in the incubation solutions drives to a reduction of the iodide influx. These data cannot be explained by considering a simple competition between chloride and iodide, as for prodiginines; thus, another player is required. In this case, we could hypothesize that gluconate (Gluc) binds to the anionophore. Therefore, the binding scheme would be:

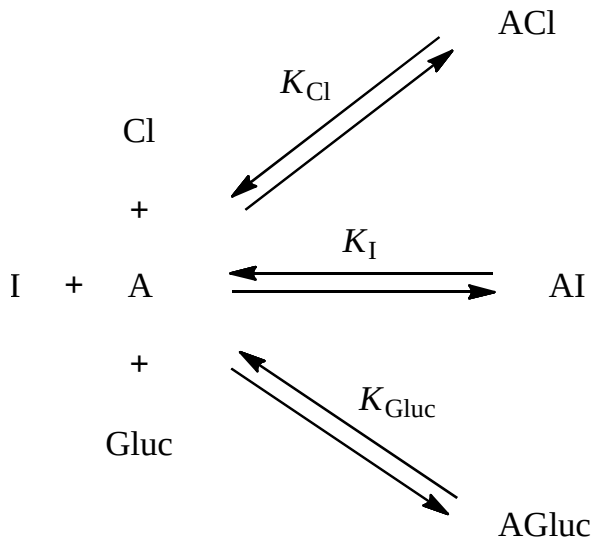

where AGluc represents the anionophore-gluconate complex. In this system the apparent dissociation constants are defined as:

$$K_{Cl}=\frac{\mathrm{Cl}\times\mathrm{A}}{\mathrm{ACl}};\ K_I=\frac{\mathrm{I}\times\mathrm{A}}{\mathrm{AI}};\ K_{Gluc}=\frac{\mathrm{Gluc}\times\mathrm{A}}{\mathrm{AGluc}};\ \mathrm{A}+\mathrm{AI}+\mathrm{ACl}+\mathrm{AGluc}=1 \quad (3)$$

where K_{Gluc} is the apparent dissociation constant of the anionophore-gluconate complex. Solving the equations in (3) for AI, we have:

$$\mathrm{AI}=\mathrm{AI}_{max}\frac{\mathrm{I}}{\mathrm{I}+\mathrm{Cl}\dfrac{K_I}{K_{Cl}}+\mathrm{Gluc}\dfrac{K_I}{K_{Gluc}}+K_I} \quad (4)$$

Thus, we measured the anionophore-driven iodide influx in cells incubated with different concentrations of NaCl, replaced by isomolar concentrations of NaGluconate. Figure 2 shows the QR value, evaluated for different concentrations of chloride, from 51 mM (and no gluconate) to zero (and 51 mM of gluconate), for each anionophore. These data were normalized to the QR value obtained in 51 mM chloride (and without gluconate). The continuous lines in Figure 2 represent the best fit of data with equation (4), and the fitting parameters are reported in Table 1. Observe that, for very high values of K_{Gluc}, the term K_I/K_{Gluc} in equation (4) tends to zero, therefore becoming identical to equation (2). Indeed, the fit of the data obtained for the prodiginine-like derivatives with equation (2) results indistinguishable from the fit with equation (4).

4. Discussion

Our experiments indicate that a large anion such as gluconate does not interfere with the iodide transport driven by our prodiginines, but it seems to reduce the iodide transport by the tambjamines (Figure 1). We have previously speculated that this result could be explained on the grounds of the fact that gluconate does not bind to the prodiginines, leaving the anionophore free to transport chloride and iodide. On the contrary, gluconate would bind to the tambjamines, competing with iodide for the anionophores, and consequently reducing the flux (Fiore et al. 2019). The data presented here support this hypothesis, since the apparent dissociation constants K_{Gluc} obtained for the prodiginine-gluconate complexes are very high, whereas those corresponding to the tambjamine-gluconate complexes are remarkably lower; interestingly, in the case of prodiginines, K_{Gluc} is about three orders of magnitude higher than K_{Cl} and K_I (Table 1). Although in our preparations we have not been able to detect the entry of gluconate into the cells nor the presence of tambjamine-gluconate complexes, we cannot exclude it a priori. The values of the apparent dissociation constants obtained for the prodiginine-halide complexes are comparable although slightly lower for the prodiginine-chloride ones, revealing that these compounds possess a somewhat higher affinity for chloride than for iodide ($K_{Cl}<K_I<K_{Gluc}$). In the case of the tambjamine derivatives, the trend is the opposite ($K_{Gluc}<K_I<K_{Cl}$), K_{Cl} being about one order of magnitude higher than K_I (Table 1). Taken together, these results suggest that prodiginines might be more effective when transporting chloride than tambjamines.

These apparent equilibrium constants are the result of various steps. We have proposed a transport mechanism for the anionophores that can be summarised as a three-step mechanism: binding of the anion – movement of the complex across the membrane – release of the anion (Cossu et al. 2018). According to this scheme, the anion flux is mainly determined by two mechanisms, the binding-unbinding of the anion and the diffusion of the anionophore-anion complex across the membrane. Therefore, the apparent dissociation constants estimated here are the product of the binding constant and the rate constant of the anionophore-anion (anion = chloride, iodide and gluconate) complex when moving across the membrane.

Given this, it was necessary to find a physical explanation for these differences by comparing some structural features of the anionophore-anion complexes. The anion binding site of these compounds is formed by three N-H groups (Figures 3 and S1) (García-Valverde et al. 2012; Hernando et al. 2018; Cossu et al. 2018; Iglesias Hernández et al. 2012; Hernando et al. 2014; Díaz de Greñu et al. 2011). There are some important differences between the prodiginines and the tambjamines' anion

binding site. Firstly, they possess a different type of ionizable N-H fragment, an azafulvene in the prodiginines, and an imine group in the tambjamines, which influences their acidity (Cossu et al. 2018). Secondly, the different geometry of the anion binding site: for the prodiginines, the angle formed by the hydrogen atoms of the three hydrogen-bond donors is, on average, of 124.5°, whereas in the case of the tambjamines such angle is about 15° wider, on average of 139.3° (see Table S1). The three hydrogen-bond donors form the putative anion binding site (see figure S1), and a dissimilar geometry of this site between the two group of anionophores may imply differnt bibnding properties. In light of these results, it seems that a large anion such as gluconate fits better in the tambjamine's binding pocket than in the prodiginine's one; this, together with the higher acidity of the former, would eventually lead to more stable complexes, which is in agreement with the values of K_{Gluc} (Table 1). Even so, the different wideness of the binding site observed for the two anionophore families does not modify substantially the distances between the anion and the hydrogen atoms of the N-H fragments, yielding an average of 2.4 to 2.6 Å for the prodiginines and 2.3 to 2.7 Å for the tambjamines (see Table S1).

We speculate that gluconate is not transported by prodiginines, as reported elsewhere (Wu et al. 2016), but we cannot exclude that they may transport gluconate at a very slow rate. Conversely, tambjamines may probably carry gluconate across the membrane at a relatively high rate. Further experiments to determine the actual gluconate transport are necessary to confirm this hypothesis.

The results obtained here imply that tambjamines could transport relatively large hydrophilic anions, such as gluconate, and be less efficient when transporting chloride. This could have an important implication both for the selection of apparently impermeable anions in the design of experiments to describe the anionophore mechanism and for the development of compounds to be used for biological purposes, as the transport of large anions is not always desired for such biological applications.

Acknowledgments. This work has received funding from the European Union's Horizon 2020 research and innovation program under grant agreement No 667079.

References

Barone, Vincenzo, and Maurizio Cossi. 1998. "Quantum Calculation of Molecular Energies and Energy Gradients in Solution by a Conductor Solvent Model." *The Journal of Physical Chemistry A* 102 (11): 1995–2001. https://doi.org/10.1021/jp9716997.

Carreira-Barral, Israel, Carlos Rumbo, Marcin Mielczarek, Daniel Alonso-Carrillo, Enara Herran, Marta Pastor, Angel Del Pozo, María García-Valverde, and Roberto Quesada. 2019. "Small Molecule Anion Transporters Display in Vitro Antimicrobial Activity against Clinically Relevant Bacterial Strains." *Chemical Communications* 55 (68): 10080–83. https://doi.org/10.1039/C9CC04304G.

Carté, Brad, and D. John Faulkner. 1986. "Role of Secondary Metabolites in Feeding Associations between a Predatory Nudibranch, Two Grazing Nudibranchs, and a Bryozoan." *Journal of Chemical Ecology* 12 (3): 795–804. https://doi.org/10.1007/BF01012111.

Cossi, Maurizio, Nadia Rega, Giovanni Scalmani, and Vincenzo Barone. 2003. "Energies, Structures, and Electronic Properties of Molecules in Solution with the C-PCM Solvation

Model." *Journal of Computational Chemistry* 24 (6): 669–81. https://doi.org/10.1002/jcc.10189.

Cossu, Claudia, Michele Fiore, Debora Baroni, Valeria Capurro, Emanuela Caci, María García-Valverde, Roberto Quesada, and Oscar Moran. 2018. "Anion-Transport Mechanism of a Triazole-Bearing Derivative of Prodigiosine: A Candidate for Cystic Fibrosis Therapy." *Frontiers in Pharmacology* 9: 852. https://doi.org/10.3389/fphar.2018.00852.

Davis, Jeffery T., Oluyomi Okunola, and Roberto Quesada. 2010. "Recent Advances in the Transmembrane Transport of Anions." *Chemical Society Reviews* 39 (10): 3843–62. https://doi.org/10.1039/B926164H.

Díaz de Greñu, Borja, Paulina Iglesias Hernández, Margarita Espona, David Quiñonero, Mark E. Light, Tomás Torroba, Ricardo Pérez-Tomás, and Roberto Quesada. 2011. "Synthetic Prodiginine Obatoclax (GX15-070) and Related Analogues: Anion Binding, Transmembrane Transport, and Cytotoxicity Properties." *Chemistry – A European Journal* 17 (50): 14074–83. https://doi.org/10.1002/chem.201101547.

Fiore, Michele, Claudia Cossu, Valeria Capurro, Cristiana Picco, Alessandra Ludovico, Marcin Mielczarek, Israel Carreira Barral, et al. 2019. "Small Molecule-Facilitated Anion Transporters in Cells for a Novel Therapeutic Approach to Cystic Fibrosis." *British Journal of Pharmacology* 176 (11): 1764–79. https://doi.org/10.1111/bph.14649.

Frisch, M. J., G. W. Trucks, H. B. Schlegel, G. E. Scuseria, M. A. Robb, J. R. Cheeseman, G. Scalmani, et al. 2016. *Gaussian 16 Rev. B.01*. Wallingford, CT.

Gale, Philip A., Jeffery T. Davis, and Roberto Quesada. 2017. "Anion Transport and Supramolecular Medicinal Chemistry." *Chemical Society Reviews* 46 (9): 2497–2519. https://doi.org/10.1039/C7CS00159B.

Galietta, Luis J. V., Peter M. Haggie, and A. S. Verkman. 2001. "Green Fluorescent Protein-Based Halide Indicators with Improved Chloride and Iodide Affinities." *FEBS Letters* 499 (3): 220–24. https://doi.org/10.1016/S0014-5793(01)02561-3.

García-Valverde, María, Ignacio Alfonso, David Quiñonero, and Roberto Quesada. 2012. "Conformational Analysis of a Model Synthetic Prodiginine." *The Journal of Organic Chemistry* 77 (15): 6538–44. https://doi.org/10.1021/jo301008c.

Hernando, Elsa, Valeria Capurro, Claudia Cossu, Michele Fiore, María García-Valverde, Vanessa Soto-Cerrato, Ricardo Pérez-Tomás, Oscar Moran, Olga Zegarra-Moran, and Roberto Quesada. 2018. "Small Molecule Anionophores Promote Transmembrane Anion Permeation Matching CFTR Activity." *Scientific Reports* 8 (1): 2608. https://doi.org/10.1038/s41598-018-20708-3.

Hernando, Elsa, Vanessa Soto-Cerrato, Susana Cortés-Arroyo, Ricardo Pérez-Tomás, and Roberto Quesada. 2014. "Transmembrane Anion Transport and Cytotoxicity of Synthetic Tambjamine Analogs." *Organic & Biomolecular Chemistry* 12 (11): 1771–78. https://doi.org/10.1039/C3OB42341G.

Iglesias Hernández, Paulina, Daniel Moreno, Anatalia Araujo Javier, Tomás Torroba, Ricardo Pérez-Tomás, and Roberto Quesada. 2012. "Tambjamine Alkaloids and Related Synthetic Analogs: Efficient Transmembrane Anion Transporters." *Chemical Communications* 48 (10): 1556–58. https://doi.org/10.1039/c1cc11300c.

Rapoport, Henry., Holden, K.G., 1962. The Synthesis of Prodigiosin. J. Am. Chem. Soc. 84, 635–642. https://doi.org/10.1021/ja00863a026

Wu, Xin, Luke W. Judd, Ethan N. W. Howe, Anne M. Withecombe, Vanessa Soto-Cerrato, Hongyu Li, Nathalie Busschaert, et al. 2016. "Nonprotonophoric Electrogenic Cl^- Transport Mediated by Valinomycin-like Carriers." *Chem* 1 (1): 127–46.

https://doi.org/10.1016/j.chempr.2016.04.002.

Yip, Chee-Hoo, Orr Yarkoni, James Ajioka, Kiew-Lian Wan, and Sheila Nathan. 2019. “Recent Advancements in High-Level Synthesis of the Promising Clinical Drug, Prodigiosin.” *Applied Microbiology and Biotechnology* 103 (4): 1667–80. https://doi.org/10.1007/s00253-018-09611-z.

Table 1. Results of the fitting of the data presented in Figure 2. AI_{max} is the expected maximum iodide influx; K_I, K_{Cl} and K_{Gluc} are the apparent dissociation constants (expressed in mM) for the iodide, chloride and gluconate complexes, respectively. Data represents the fitting results ± the standard deviation of each parameter.

	EH130	**OBX**	**PRG**	**MM3**	**RQ363**
$\mathbf{AI_{max}}$	3.15 ± 0.14	2.06 ± 0.03	1.74 ± 0.01	1.10 ± 0.01	1.11 ± 0.01
$\boldsymbol{K_I}$	4.59 ± 0.68	3.79 ± 0.22	4.36 ± 0.16	1.98 ± 0.07	2.11 ± 0.07
$\boldsymbol{K_{Cl}}$	2.47 ± 0.43	2.76 ± 0.18	4.02 ± 0.16	10.68 ± 2.63	20.69 ± 9.96
$\boldsymbol{K_{Gluc}}$	> 1000	> 1000	> 1000	0.64 ± 0.02	0.57 ± 0.02

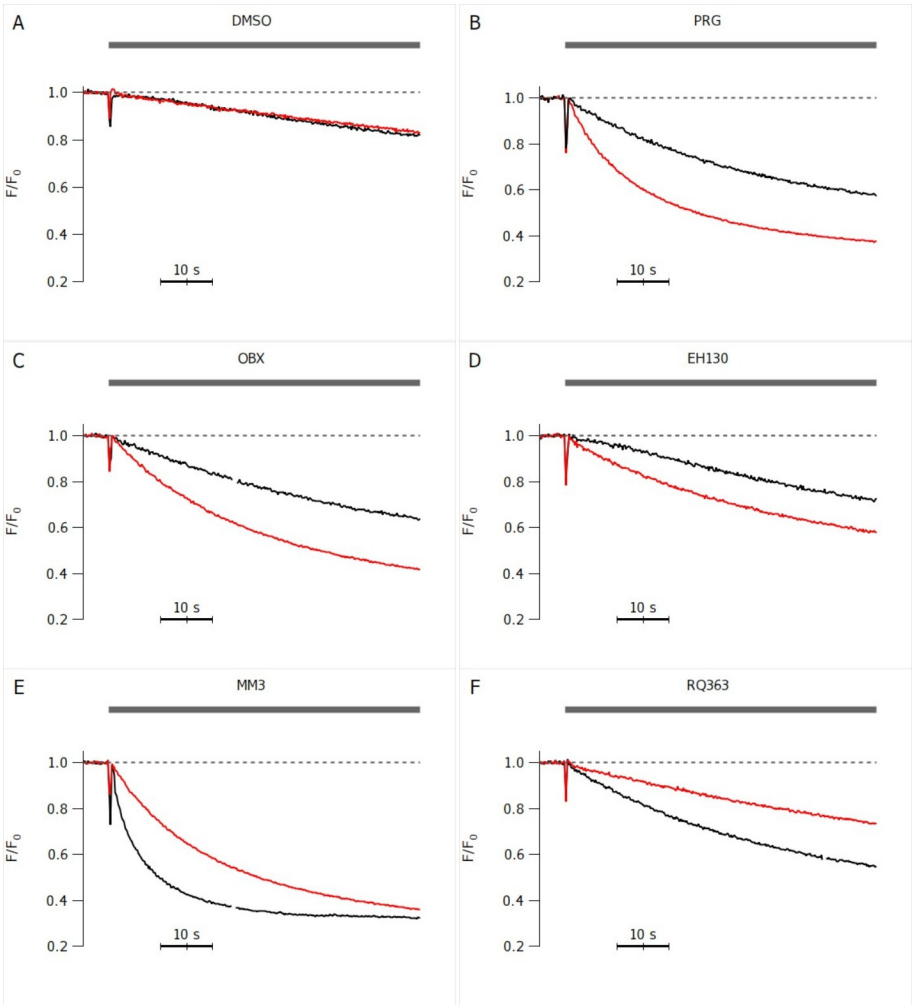

Figure 1. Iodide influx assay in FRT cells. Time course of the fluorescence decay of cells incubated with 2 µM solutions of the prodiginines (B, C, D) and the tambjamines (E, F) at different concentrations of NaGluconate after iodide injection: black 0 mM, red 51 mM. Cells treated with vehicle were used as control (A).

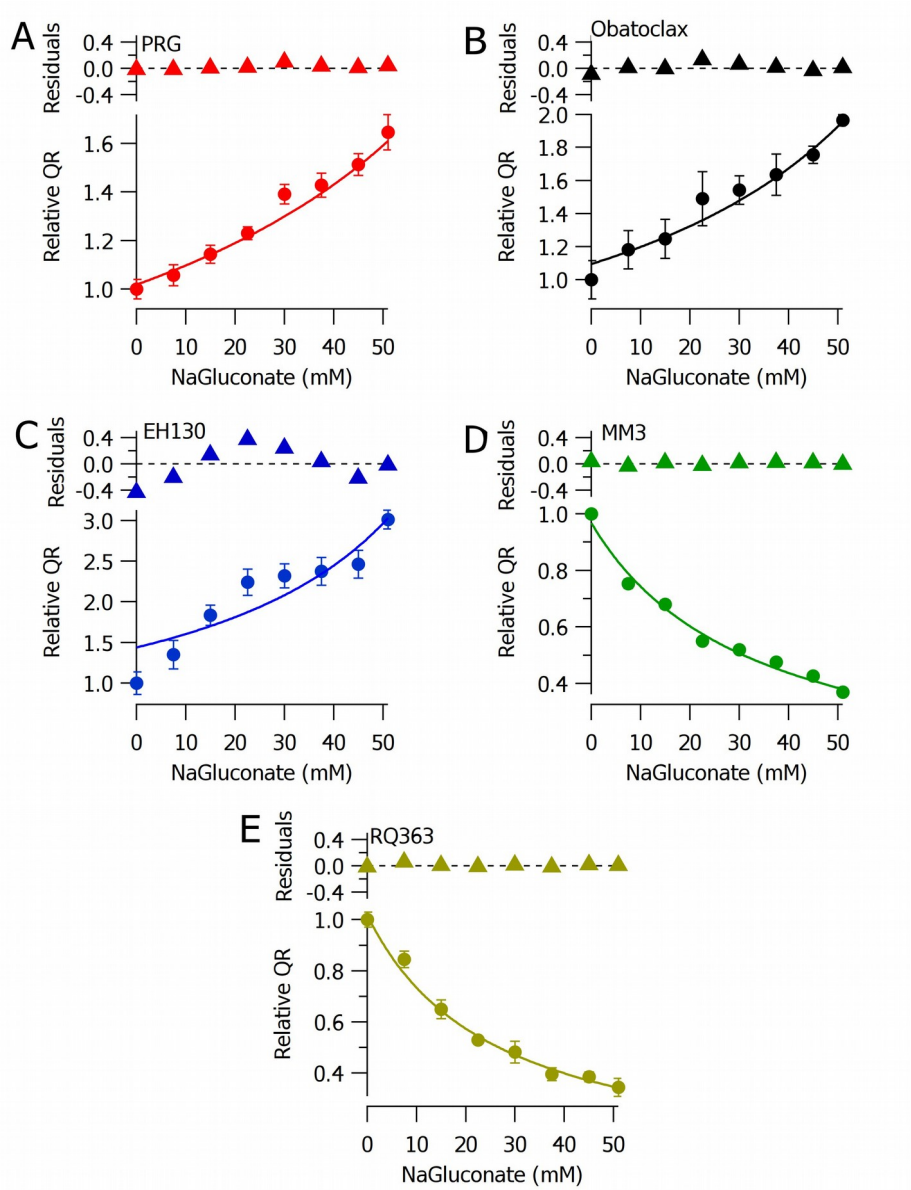

Figure 2. Quenching rate (QR) values of YFP plotted against the NaGluconate and NaCl concentrations for the prodiginines: Prodigiosine (PRG) **A**, Obatoclax (OBX) **B**, EH130 **C**, and tambjamines: MM3 **D** and RQ363 **E**. Data are normalized to QR measurement with the maximum concentration of chloride (51 mM NaCl and 0 mM NaGluconate after NaI injection); residuals are shown at the top of each graph.

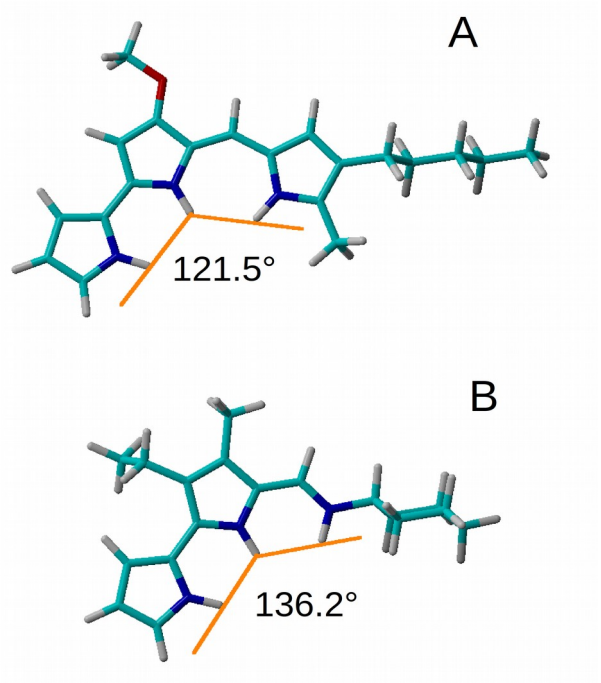

Figure 3. The optimized structures of PRG (**A**) and MM3 (**B**) obtained by computational calculations in an aqueous environment. The orange lines indicate the position of the anion binding site for each compound. The angle formed by the hydrogen atoms of the three N-H fragments is indicated in each panel.

Supplementary material for online publication only

Click here to download Supplementary material for online publication only: EJP-suppl.pdf

***Author Agreement**

All authors of this work have seen and approved the final version of the manuscript being submitted. We warrant that the article is the authors' original work, hasn't received prior publication and isn't under consideration for publication elsewhere.

Figure1

Click here to download high resolution image

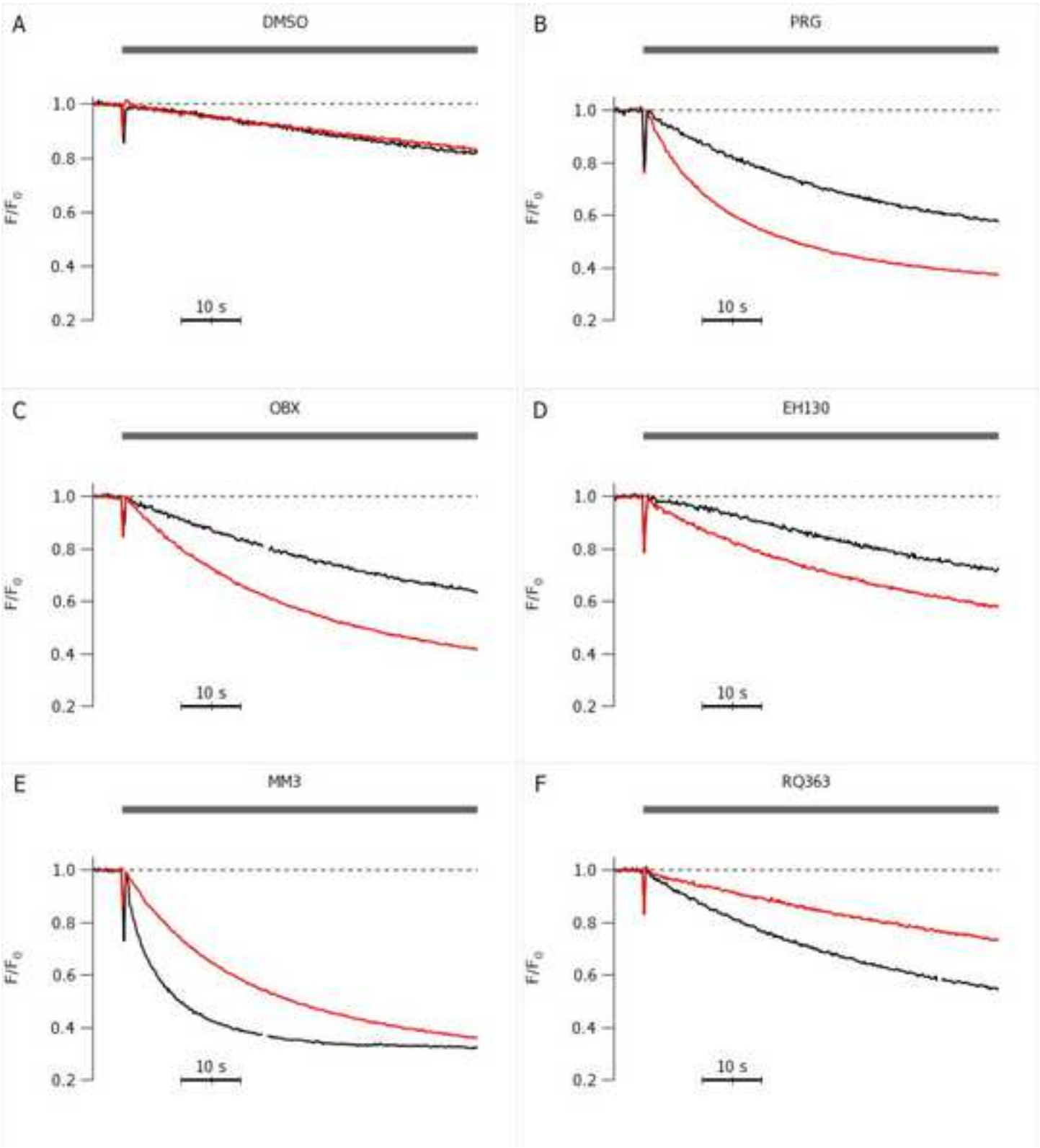

Figure2

Click here to download high resolution image

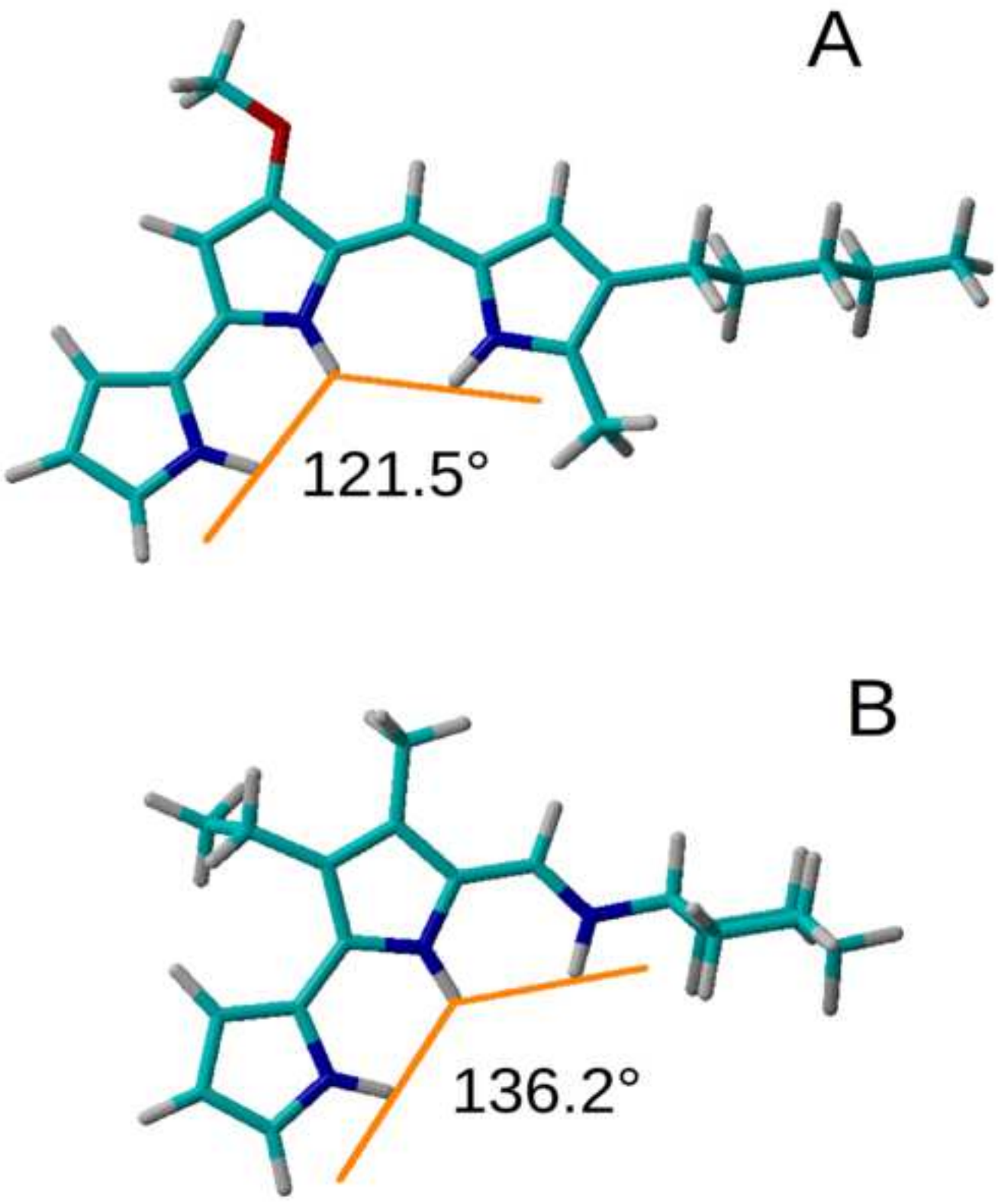

Figure1S

Click here to download high resolution image